



## Review

# Structural analysis and binding sites of inhibitors targeting the CD47/SIRP $\alpha$ interaction in anticancer therapy



Bo Huang<sup>a</sup>, Zhaoshi Bai<sup>c,\*</sup>, Xinyue Ye<sup>b</sup>, Chenyu Zhou<sup>b</sup>, Xiaolin Xie<sup>a,b</sup>, Yuejiao Zhong<sup>c</sup>, Kejiang Lin<sup>a,\*</sup>, Lingman Ma<sup>a,b,\*</sup>

<sup>a</sup> Department of Medicinal Chemistry, School of Pharmacy, China Pharmaceutical University, 639 Longmian Road, Nanjing, Jiangsu 211198, China

<sup>b</sup> School of Life Science and Technology, China Pharmaceutical University, 639 Longmian Road, Nanjing, Jiangsu 211198, China

<sup>c</sup> Jiangsu Cancer Hospital & Jiangsu Institute of Cancer Research & the Affiliated Cancer Hospital of Nanjing Medical University, Baiziting 42, Nanjing, Jiangsu 210009, China

## ARTICLE INFO

## Article history:

Received 30 June 2021

Received in revised form 18 September 2021

Accepted 30 September 2021

Available online 01 October 2021

## Keywords:

Immunotherapy

CD47/SIRP $\alpha$

Crystal structure

Inhibitor

Computer-aided drug discovery

Hot spot

## ABSTRACT

Cluster of differentiation 47 (CD47)/signal regulatory protein alpha (SIRP $\alpha$ ) is a negative innate immune checkpoint signaling pathway that restrains immunosurveillance and immune clearance, and thus has aroused wide interest in cancer immunotherapy. Blockade of the CD47/SIRP $\alpha$  signaling pathway shows remarkable antitumor effects in clinical trials. Currently, all inhibitors targeting CD47/SIRP $\alpha$  in clinical trials are biomacromolecules. The poor permeability and undesirable oral bioavailability of biomacromolecules have caused researchers to develop small-molecule CD47/SIRP $\alpha$  pathway inhibitors. This review will summarize the recent advances in CD47/SIRP $\alpha$  interactions, including crystal structures, peptides and small molecule inhibitors. In particular, we have employed computer-aided drug discovery (CADD) approaches to analyze all the published crystal structures and docking results of small molecule inhibitors of CD47/SIRP $\alpha$ , providing insight into the key interaction information to facilitate future development of small molecule CD47/SIRP $\alpha$  inhibitors.

© 2021 The Author(s). Published by Elsevier B.V. on behalf of Research Network of Computational and Structural Biotechnology. This is an open access article under the CC BY-NC-ND license (<http://creativecommons.org/licenses/by-nc-nd/4.0/>).

## Contents

1. Introduction	5495
2. Structures of CD47/SIRP $\alpha$ complexes and cocrystal structures of monoclonal antibodies	5496
3. Bioactive peptide inhibitors blocking the CD47/SIRP $\alpha$ interaction	5497
3.1. CD47-targeted peptides	5498
3.1.1. Pep-20 and its derivatives	5498
3.1.2. Rs-17	5498
3.2. SIRP $\alpha$ -targeted peptides	5498
3.2.1. d4-2	5498
3.2.2. Sp5	5498
3.3. CADD guides the design of peptide inhibitors	5498
4. Small molecule inhibitors blocking the CD47/SIRP $\alpha$ interaction	5498
4.1. NCGC00138783 and its derivatives	5498
4.2. 1,2,4-oxadiazole compounds	5499
4.3. CADD guides the design of small molecule inhibitors	5501
5. Summary and outlook	5501
CRedit authorship contribution statement	5501
Declaration of Competing Interest	5502

\* Corresponding authors at: Jiangsu Cancer Hospital & Jiangsu Institute of Cancer Research & the Affiliated Cancer Hospital of Nanjing Medical University, Baiziting 42, Nanjing, Jiangsu 210009, China (Z. Bai); Department of Medicinal Chemistry, School of Pharmacy, China Pharmaceutical University, 639 Longmian Road, Nanjing, Jiangsu 211198, China (K. Lin); School of Life Science and Technology, China Pharmaceutical University, 639 Longmian Road, Nanjing, Jiangsu 211198, China (L. Ma).

E-mail addresses: [baizhaoshi23@126.com](mailto:baizhaoshi23@126.com) (Z. Bai), [link@cpu.edu.cn](mailto:link@cpu.edu.cn) (K. Lin), [1620174416@cpu.edu.cn](mailto:1620174416@cpu.edu.cn) (L. Ma).

<https://doi.org/10.1016/j.csbj.2021.09.036>

2001-0370/© 2021 The Author(s). Published by Elsevier B.V. on behalf of Research Network of Computational and Structural Biotechnology.

This is an open access article under the CC BY-NC-ND license (<http://creativecommons.org/licenses/by-nc-nd/4.0/>).

Acknowledgements ..... 5502  
 References ..... 5502

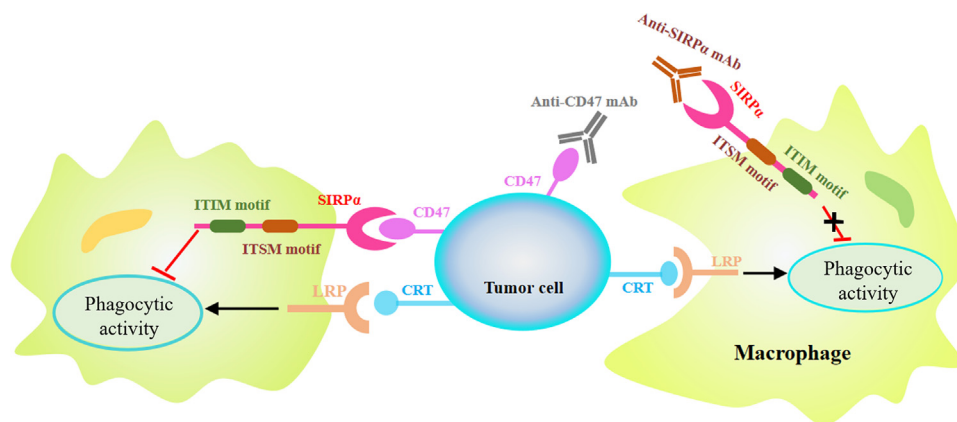
**1. Introduction**

Currently, the high morbidity and mortality of tumors remain a major challenge to the effectiveness of cancer treatment even though a series of anticancer drugs have been developed based on different treatment strategies [1]. Cancer immunotherapy, which aims to improve antitumor immune responses with fewer off-target effects than chemotherapies and other agents that directly kill cancer cells, provides an alternative strategy to treat cancer through the immune system rather than the tumor itself [2] and is an exciting area in current cancer research [3,4]. This novel therapy, including immune checkpoint blockade, adoptive cellular therapy and cancer vaccinology [5], has led to a growing number of immunotherapy drug approvals, with numerous treatments in clinical and preclinical development [3].

Herein, the immune checkpoint plays a central role in tissue homeostasis self-reactivity and autoimmunity, which targets the innate and adaptive immune systems [6], and is the signal recognition factor for immunosurveillance in immune cells [7]. However, some tumor cells evade immune clearance by modulating signal recognition between immune cells and tumor cells; thus, immune checkpoint blockade is the main promising system in immunotherapy [8,9]. To date, the blockade of two well-known adaptive immune system checkpoints, cytotoxic T-lymphocyte-associated antigen 4 (CTLA4) and programmed cell death protein 1 (PD1), has led to the generation of several immune checkpoint inhibitors that have been used for treating multiple cancers [10–13]; however, an unsatisfactory overall response rate, tumor heterogeneity, drug resistance and rapid progression after therapy in patients are some of the challenges of inhibiting adaptive immune checkpoints [14–17].

Interestingly, in addition to adaptive immunity, innate immune processes may also provide a good direction for cancer immunotherapy. Recently, CD47, which is one of the most attractive innate immune checkpoint regulators because of its inhibitory effect on the activation of macrophages and other myeloid cells against tumor, brings new hope to cancer patients. It belongs to the immunoglobulin (Ig) superfamily and is ubiquitously-expressed on all normal cells but overexpressed on hematological and solid malignancy cancer cell membranes [18–21]. As a highly

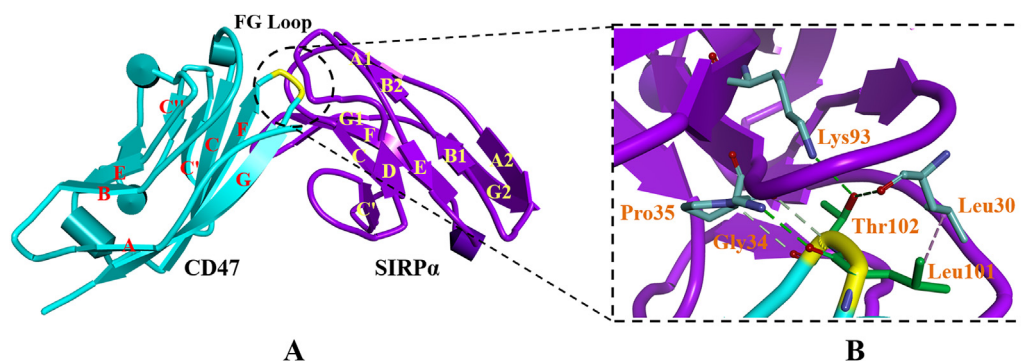
glycosylated transmembrane protein, CD47 consists of an extracellular amino terminal IgV-like domain, five membrane-spanning segments that are highly hydrophobic and a hydrophilic cytoplasmic C-terminus that is 3–6 amino acids long [22], and it interacts with the NH<sub>2</sub>-terminal V-set domain of its ligand, SIRPα [23]. SIRPα is also known as CD172a or SHPS-1 and is highly expressed on the membrane of myeloid cells, such as monocytes, macrophages, neutrophils, and dendritic cells (DCs) [10,24,25]. CD47 interacts with SIRPα, tagging it with a “self” or “do not eat” signal, to trigger an inhibitory signaling cascade through the ITIM and ITSM motifs of SIRPα, inhibiting macrophage phagocytosis (Fig. 1) [26–28]. Unfortunately, when overexpressed CD47 on the surface of solid malignancies binds to SIRPα on macrophages, this can suppress the phagocytic responses of macrophages [29]. Therefore, as a dominant macrophage checkpoint, disruption of the CD47/SIRPα pathway can induce macrophage-mediated phagocytosis of tumor cells and thus is employed when generating next-generation immunoregulatory drugs [30–32]. Currently, the gradual increase in patents with treatments targeting the CD47/SIRPα pathway clearly demonstrates the great effort being made to discover new inhibitors of this target. Consequently, some CD47/SIRPα pathway-targeting antibodies against various cancers (Table. 1), including acute myeloid leukemia (AML) [33,34], anaplastic thyroid carcinoma (ATC) [35], lymphoma [36–38], lung cancer [39,40] and breast cancer [41], have showed attractive results. For example, magrolimab (Hu5F9-G4) is an anti-CD47 monoclonal antibody that is currently undergoing phase III clinical trials, with an objective response rate of 75% in phase Ib clinical results during the treatment of myelodysplastic syndromes. ALX-148 is also a CD47 targeting antibody in phase II clinical trials whose objective responses could be observed in phase I clinical results for the treatment of patients with head and neck squamous cell carcinoma. It is undeniable that some adverse effects occur when using these antibodies therapeutically, such as the rapid target-mediated clearance, transient anemia, erythrocyte toxicity and infusion-related reactions [42], which limit their rapid development. In addition, there are certain limitations of using these antibodies, including a long half-life, poor permeability and lacking oral availability. Thus, the development of low molecular-weight inhibitors with superb pharmacokinetics and druggability is an effective strategy



**Fig. 1.** CD47/SIRPα pathway. Cell surface calreticulin (CRT) binds to low-density lipoprotein-related protein (LRP) to promote phagocytosis. CD47 can downregulate phagocytic activity by interacting with SIRPα on macrophages. Blockade of the CD47/SIRPα pathway through Anti-CD47 mAb can recover phagocytic activity of macrophage.

**Table 1**  
CD47/SIRP $\alpha$  targeting mAbs in clinical trial.

Code Name (Generic Name)	Target	Organization	Therapeutic Groups	Highest Phase
Hu5F9-G4 (Magrolimab)	CD47	Gilead	Bladder Cancer, Breast Cancer, Colorectal Cancer, Hematological Cancer, Lymphoma, Myeloid Leukemia, Non-Hodgkin's Lymphoma, Ovarian Cancer.	III
ALX-148	CD47	Alexo Therapeutics	Gastric Cancer, Head and Neck Cancer, Non-Hodgkin's Lymphoma.	II
TJC-4 (Lemzoparlimab)	CD47	AbbVie	Lymphoma, Myeloid Leukemia.	II
DSP-107	CD47	KAHR Medical	Non-Small Cell Lung Cancer.	II
IBI-188 (Letaplimab)	CD47	Innovent Biologics	Myeloid Leukemia, Non-Hodgkin's Lymphoma, Ovarian Cancer.	II
AO-176	CD47	Arch Oncology	Lymphoma, Multiple Myeloma.	II
TTI-622	CD47	Trillium Therapeutics	Lymphoma, Multiple Myeloma, Myeloid Leukemia, Non-Hodgkin's Lymphoma, Ovarian Cancer.	II
ZL-1201	CD47	ZAI Lab	Lymphoma Therapy.	I
AK-117	CD47	Akeso Biopharma	Non-Hodgkin's Lymphoma Therapy.	I
IMC-002	CD47	ImmuneOncia Therapeutics	Lymphoma.	I
SRF-231	CD47	Surface Oncology	Hematological Cancer Therapy, Lymphocytic Leukemia Therapy, Lymphoma Therapy, Multiple Myeloma Therapy.	I
CC-90002	CD47	Celgene	Myeloid Leukemia Therapy, Non-Hodgkin's Lymphoma Therapy.	I
TTI-621	CD47	Trillium Therapeutics	Hematological Cancer Therapy, Lymphocytic Leukemia Therapy, Myeloid Leukemia Therapy, Non-Hodgkin's Lymphoma Therapy.	I
GS-0189	SIRP $\alpha$	Gilead	Oncolytic Drug.	I
CC-95251	SIRP $\alpha$	Celgene	Solid Tumors.	I
FSI-189	SIRP $\alpha$	Gilead	Non-Hodgkin's Lymphoma	I
BI-765063	SIRP $\alpha$	Boehringer Ingelheim	Solid Tumors Therapy	I

**Fig. 2.** Structure of the CD47/SIRP $\alpha$  d1 complex and the interaction between the FG loop and SIRP $\alpha$  d1. (A) Overview of the CD47/SIRP $\alpha$  d1 complex. CD47 is colored cyan, the FG loop is colored yellow, and SIRP $\alpha$  d1 is colored purple. (B) The FG loop/SIRP $\alpha$  d1 interaction. The residues of the FG loop are colored green, and the interacting residues of SIRP $\alpha$  d1 are colored navy. (For interpretation of the references to colour in this figure legend, the reader is referred to the web version of this article.)**Table 2**  
Contact residues of CD47 and SIRP $\alpha$  d1 (distances <5.0 Å).

CD47 contact residue	CD47 residue location	SIRP $\alpha$ contact residue	SIRP $\alpha$ residue location
Gln <sup>1</sup> , Lys <sup>6</sup>	A loop	Ile <sup>30</sup> , Gly <sup>34</sup> , Pro <sup>35</sup>	B2C
Asn <sup>27</sup> , Glu <sup>29</sup> , Glu <sup>35</sup>	BC loop	Gln <sup>52</sup> , Lys <sup>53</sup> , Glu <sup>54</sup>	C'D loop
Tyr <sup>37</sup> , Lys <sup>39</sup>	C strand	Ser <sup>66</sup> , Thr <sup>67</sup> , Arg <sup>69</sup>	DE loop
Asp <sup>46</sup>	C' strand	Lys <sup>93</sup>	F strand
Glu <sup>97</sup> , Glu <sup>100</sup>	F strand	Lys <sup>96</sup> , Gly <sup>97</sup> , Ser <sup>98</sup> , Asp <sup>100</sup>	FG1 strand
Leu <sup>101</sup> , Thr <sup>102</sup>	FG loop		
Arg <sup>103</sup> , Glu <sup>104</sup> , Glu <sup>106</sup>	G strand		

and research focus to overcome the limitations of therapeutic antibodies [43].

Because the development of small molecule inhibitors of the CD47/SIRP $\alpha$  interaction has been slower than the development of antibody treatments, research on the CD47/SIRP $\alpha$  pathway is crucial. Currently, high-throughput screening and computer-aided drug design (CADD) are common approaches in the discovery of small molecule inhibitors [44–48]. CADD is a molecular design method based on computational chemistry [49,50] and can help

to produce valuable information on target proteins, lead compounds and protein–ligand interactions for rational drug design. Thus, CADD is used both to analyze hot spots of target proteins and protein–ligand interactions model for further drug discovery. In this review, we have employed the “View Interactions” tool in CADD to analyze the hot spots of CD47 and SIRP $\alpha$  based on their cocrystal structures. Subsequently, “LibDock” in CADD was further applied to predict the key interacting amino acids of CD47 and SIRP $\alpha$  from a small molecule inhibitor docking experiment. In addition, some of the peptides and small molecule inhibitors that have been reported to block the CD47/SIRP $\alpha$  interaction in fundamental research studies have been summarized, and their structure–activity relationships have been analyzed and compared to guide the discovery and design of new inhibitors blocking the CD47/SIRP $\alpha$  interaction with superb pharmacokinetics and druggability.

## 2. Structures of CD47/SIRP $\alpha$ complexes and cocrystal structures of monoclonal antibodies

The first high-resolution crystallographic structure of the CD47/SIRP $\alpha$  d1 complex (the ligand-binding domain) was published by

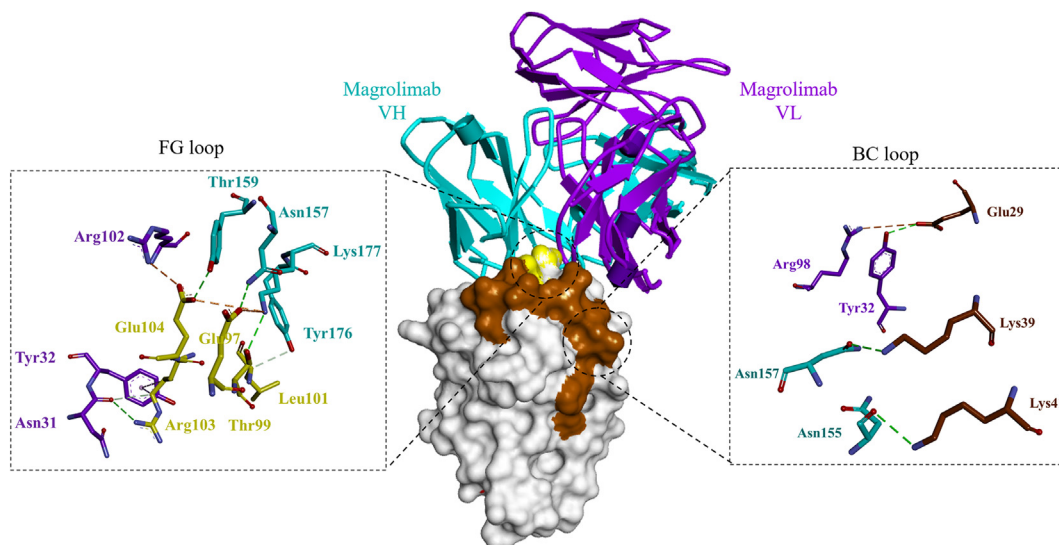


**Fig. 3.** Structure of the Magrolimab/CD47 complex. The FG and BC loops of CD47 are colored yellow and brown, respectively. The residues in the VH of magrolimab are colored cyan, and the residues in the VL of magrolimab are colored purple. The green dashed lines indicate hydrogen bond formation. (For interpretation of the references to colour in this figure legend, the reader is referred to the web version of this article.)

Hatherley et al. in 2008 and the identifier of this complex in Protein Data Bank is 2JJT (PDB ID: 2JJT) [51]. Within the crystal, CD47 and SIRP $\alpha$  d1 form a 1:1 stoichiometry complex. The CD47 and SIRP $\alpha$  d1 molecules are interdigitated to each other so that their interaction is mainly mediated by loops at the intracellular side, which is consistent with what had been proposed by other authors based on their analyses [52]. The CD47/SIRP $\alpha$  d1 interaction interface is mainly formed of four N-terminal loops of the SIRP $\alpha$  d1 domain and the FG loop of CD47, which embeds into the cavity on the surface of SIRP $\alpha$  d1. Thr<sup>102</sup> of the FG loop inserts deep into SIRP $\alpha$  d1 (Fig. 2, produced by Discovery Studio2019). The hot spot residue-mediated polar interactions on CD47 comprise Glu<sup>97</sup>, Thr<sup>99</sup>, Glu<sup>100</sup>, Arg<sup>103</sup>, Glu<sup>104</sup>, and Glu<sup>106</sup>. Among them, Glu<sup>104</sup> and Glu<sup>106</sup> of CD47 form hydrogen bonds with SIRP $\alpha$  (Table 2), and the BC loop surrounding the FG loop interacts with the wide edge of the SIRP $\alpha$  groove. Comparative analysis of the CD47/SIRP $\alpha$  d1 complex structures with isolated structures of CD47 and SIRP $\alpha$  demonstrates that complex formation slightly impacts the backbone of CD47. In contrast, the complex formation rearranges the CD47-interacting loops in SIRP $\alpha$  d1. In addition, Weiskopf et al. reported the high-affinity SIRP $\alpha$  variant FD6/CD47 complex in 2013 [53]. The root mean square deviation (RMSD) between the FD6/CD47 complex and the wild-type SIRP $\alpha$ /CD47 complex is 0.61 Å. FD6 and wild-type SIRP $\alpha$  interact with the overlapping CD47 epitope. However, key mutations in the C'D loop of FD6 may promote the interaction between Ala<sup>53</sup> and glutamic acids on CD47 [53].

To date, four complex crystal structures of CD47/mAbs have been reported. They are the CD47/magrolimab complex (PDB ID: 5IWL) [30], CD47/B6H12.2 complex (PDB ID: 5TZU) [54], CD47/C47B222 complex (PDB ID: 5TZ2) [54], and CD47/C47B161 complex (PDB ID: 5TZT) [54]. Magrolimab, also known as Hu5F9-G4, is an IgG4 antibody and can form a Hu5F9-G4 diabody/CD47-ECD complex with the CD47 extracellular domain (CD47-ECD). Hu5F9-G4 employs VH and VL to cover the CD47-ECD surface area with 365 Å<sup>2</sup> and 310 Å<sup>2</sup>, respectively. Superposition of the CD47/magrolimab complex and CD47/SIRP $\alpha$  complex reveals that their surface interaction involves similar epitopes on CD47, including the BC and FG loops. Specifically, the CDR loops of magrolimab form 11 hydrogen bonds with the CD47-ECD surface (Fig. 3, produced by Discovery Studio2019). Moreover, the

**Table 3**

Sequences of bioactive peptides inhibitors blocking the CD47/SIRP $\alpha$  interaction.

Code Name (Generic Name)	Target	Organization	Sequence
RS-17 [58]	CD47	China Pharmaceutical University	RRYKQDGGWSHWSPWSS-NH2
Pep-20 [55]	CD47	Sun Yat-sen University and Zhengzhou University	AWSATWSNYWRH
D4-2 [59,60]	SIRP $\alpha$	Kobe University	Ac-yRYSAVYSIHPSWCC-NH2
SP5 [62]	SIRP $\alpha$	Zhengzhou University	CTQDAWHIC

crystal structures of the CD47-B6H12.2, CD47-C47B222, and CD47-C47B161 complexes demonstrate that the interaction interface of all three antibodies overlaps with the SIRP $\alpha$  binding epitope regions on the FG loop of CD47. Thus, these complex structures demonstrate that the FG loop of CD47 is a key component of the interaction, indicating that the FG loop may become a potential target for further structure-based drug design.

Magrolimab mainly binds to N-terminal pyroglutamate of CD47 which is critical for CD47/SIRP $\alpha$  interaction and magrolimab binds to the BC and FG loops, which are highly overlapping epitopes with SIRP $\alpha$  [55,56]. Analogously, the common binding area of B6H12.2, C47B161 and C47B222 is the CC' and FG loops on CD47. According to these findings, the N-terminal pyroglutamate and the BC, CC' and FG loops can be viewed as potential binding areas for subsequent structure-based drug design, and Tyr<sup>37</sup>, Asp<sup>46</sup>, Glu<sup>97</sup>, Glu<sup>100</sup> and Glu<sup>106</sup> may be developed into binding sites for inhibitors targeting CD47. Additionally, the loops of SIRP $\alpha$  undergo structural changes in the interaction with CD47, which indicates that C'D, DE, and FG loops may be possible targets. Among these loops, Glu<sup>54</sup>, Gly<sup>55</sup>, Ser<sup>66</sup> and Ser<sup>98</sup> undergo considerable movement, implying that these residues play crucial roles in the interaction and may act as binding sites for designing future SIRP $\alpha$  inhibitors.

### 3. Bioactive peptide inhibitors blocking the CD47/SIRP $\alpha$ interaction

The development of non-antibodies with succinct synthesis and lower modification cost has led to the discovery of RS-17, Pep-20,



D4-2, and SP5. All four peptides, whose sequences are listed in Table 3, can directly block the CD47/SIRP $\alpha$  interaction. RS-17 and Pep-20 block the CD47/SIRP $\alpha$  interaction by binding to CD47, while D4-2 and SP5 can bind to SIRP $\alpha$  to disrupt the CD47/SIRP $\alpha$  interaction.

### 3.1. CD47-targeted peptides

#### 3.1.1. Pep-20 and its derivatives

In 2020, Pep-20 and its derivatives that have comparable affinity to the CD47/SIRP $\alpha$  interaction were identified by Wang et al. using a subtractive phage biopanning strategy [57]. The  $K_d$  values of pep-20 binding to human and mouse CD47 are  $2.91 \pm 1.04 \mu\text{M}$  and  $3.63 \pm 1.71 \mu\text{M}$ , respectively, which are close to that of cognate SIRP $\alpha$  [58,59]. In addition, a human CD47/SIRP $\alpha$  blocking assay also revealed that pep-20 exhibited an  $\text{IC}_{50}$  of  $24.56 \mu\text{M}$  with the anti-CD47 antibody (B6H12), which served as a positive control. Pep-20 remarkably enhances the phagocytosis of MCF7 (human breast tumor cell lines), HT29 (human colon tumor cell lines) and Jurkat (human leukemia cell lines) and exhibits an enhancement of phagocytosis similar to that of the positive control (B6H12). Excitingly, the injection of pep-20 at a dose of 2 mg/kg daily in mice had no obvious influence on the reduction in the number of red blood cells, which is a common toxicity effect of CD47/SIRP $\alpha$  blockade [57]. Furthermore, after replacing three terminal residues of pep-20 with D-amino acids, the obtained peptide pep-20-D12 significantly improved stability without a functional decrease compared with pep-20, accompanied by an intravenous elimination  $T_{1/2}$  that increased by tenfold compared with pep-20. Pep-20-D12 remarkably slows tumor progression, and the combination treatment of pep-20-D12 and IR shows tumor growth regression in colon tumor (MC38 cells)-bearing mice [57]. A subsequent docking model and alanine substitution experiment of pep-20/CD47 revealed that Phe<sup>4</sup>, Glu<sup>104</sup> and Glu<sup>106</sup> of CD47 are key positions for inhibitors targeting CD47. These findings provide valuable information of CD47 binding sites and the key structure of pep-20 for small-molecule inhibitor design.

#### 3.1.2. Rs-17

Additionally, Xu et al. from China Pharmaceutical University discovered RS-17 in 2020 [60]. The  $K_d$  value of RS-17 binding to the CD47 protein was  $3.85 \pm 0.79 \text{ nM}$ . At a concentration of  $20 \mu\text{g/ml}$ , RS-17 effectively binds to CD47 of SCC-13 (human epidermal squamous tumor cells) and HepG2 (human liver tumor cells) with corresponding binding rates of 55.5% and 71.2%, respectively; thus, the phagocytic efficiency of macrophages against HepG2 cells was greatly improved, showing a half phagocytic index of B6H12. Moreover, an *in vivo* assay demonstrated that the weight loss and tumor volume increase in liver tumor-bearing mice were similar between RS-17 and B6H12 and that RS-17 effectively inhibited tumor growth in liver tumor-bearing mice.

### 3.2. SIRP $\alpha$ -targeted peptides

#### 3.2.1. d4-2

Hazama et al. utilized random nonstandard peptides integrated discovery (RaPID) system, which combines flexizyme-assisted genetic code reprogramming and mRNA display to obtain macrocyclic peptides of interest, to design and gain anti-SIRP $\alpha$  peptides L4-4, D4-1, D4-2 and D4-4 [61,62]. Among these peptides, D4-2 shows comprehensive high binding affinity to SIRP $\alpha$  of C57BL/6 and NOD mouse strains with corresponding  $K_d$  values of 10 nM and 8.22 nM, respectively. D4-2 evidently blocked the mCD47-Fc/NOD SIRP $\alpha$  interaction in a dose-dependent manner in HEK293A (human embryonic kidney cells) cells with an  $\text{IC}_{50}$  value

of 0.180 mM. The crystal structure of the D4-2/NOD SIRP $\alpha$  complex shows that the interaction area of D4-2/NOD SIRP $\alpha$  occupies  $976.5 \text{ \AA}^2$ . Arg<sup>2</sup>, Ser<sup>4</sup>, Ala<sup>5</sup>, Val<sup>6</sup>, Ile<sup>9</sup>, His<sup>10</sup>, Pro<sup>11</sup>, Ser<sup>12</sup>, Trp<sup>13</sup> and Gly<sup>15</sup> of D4-2 form hydrogen bonds with IgV-NOD SIRP $\alpha$ , and Arg<sup>2</sup> of D4-2 forms a salt bridge with Asp<sup>84</sup> of IgV-NOD SIRP $\alpha$ . Ala<sup>5</sup> and Pro<sup>11</sup> of D4-2 form hydrophobic interactions with Phe<sup>51</sup> and Phe<sup>56</sup> of IgV-NOD SIRP $\alpha$ . All these residues stabilize the cyclic structure of D4-2 and mediate the binding of D4-2 to IgV-NOD SIRP $\alpha$ . Further crystal structure comparison shows that the binding of D4-2 to Phe<sup>56</sup> and Ala<sup>65</sup> in the C'E loop of IgV-NOD SIRP $\alpha$ , which are key residues controlling the interaction with CD47, changes the conformation and induces the inhibition of the CD47/IgV-NOD SIRP $\alpha$  interaction [63].

#### 3.2.2. Sp5

In addition to D4-2, a series of macrocyclic peptides binding to SIRP $\alpha$ , including SP1 to SP6, were also developed in 2020 by Xu et al from Zhengzhou University [64]. Among these, SP4 and SP5 display higher affinity to SIRP $\alpha$  with  $K_d$  values of  $0.85 \mu\text{M}$  and  $0.38 \mu\text{M}$  and block the SIRP $\alpha$ /CD47 interaction in a dose-dependent manner in CHO-K1-hSIRP $\alpha$  cells. SP5 ( $200 \mu\text{M}$ ) not only effectively promotes the phagocytosis of HT29 (human colon tumor cells) by macrophages but also exhibits desirable *in vivo* efficacy by inhibiting tumor growth in colon tumor MC38 mouse model and melanoma B16-OVA mouse model.

### 3.3. CADD guides the design of peptide inhibitors

Analysis of the previously described peptides can lead to conclusions that these peptides share similar interaction areas that overlap with the epitopes in the CD47/SIRP $\alpha$  interaction area. For example, Pep-20 occupies Phe<sup>4</sup>, Glu<sup>104</sup> and Glu<sup>106</sup> of CD47 to block the D47-SIRP $\alpha$  interaction, and D4-2 binds to Phe<sup>56</sup> and Ala<sup>65</sup> of SIRP $\alpha$  to block the D47-SIRP $\alpha$  interaction. Moreover, these peptides mainly form hydrogen bonds with their receptor. Collectively, residues Phe<sup>4</sup>, Glu<sup>104</sup> and Glu<sup>106</sup> of CD47 and residues Phe<sup>56</sup> and Ala<sup>65</sup> of SIRP $\alpha$  may be developed into binding sites for structure-based CD47/SIRP $\alpha$  small molecule inhibitor design.

## 4. Small molecule inhibitors blocking the CD47/SIRP $\alpha$ interaction

### 4.1. NCGC00138783 and its derivatives

Miller et al. utilized quantitative high-throughput screening (qHTS) assays to screen NCATS chemical libraries based on time-resolved Förster resonance energy transfer (TR-FRET) and bead-based luminescent oxygen channeling assay formats (AlphaScreen), resulting in the discovery of the parent compound NCGC00138783 [65,66] whose scaffold is 2-((2-(2-(3,5-dimethyl-1H-pyrazol-4-yl) ethyl)-5,6-dihydro-[1,2,4] triazolo [1,5-c] quinazolin-5-yl) thio) butanal. This compound selectively blocks the CD47/SIRP $\alpha$  interaction without disrupting its binding to other receptors [67–69]. A novel laser scanning cytometry assay (LSC) was established to measure the cell surface binding of these compounds, and the results showed that NCGC00138783 has an  $\text{IC}_{50}$  value of  $40 \mu\text{M}$ . Further medicinal chemistry work attempting to optimize the potency and drug-like properties of NCGC00138783 led to the discovery of its derivatives (Fig. 4, produced by ChemDraw). The acyl group of NCGC00138783 is linked with a monocyclic substituted amino group and hydroxyl group to obtain a range of compounds displaying great inhibitory activity toward the CD47/SIRP $\alpha$  interaction. Among these small molecule compounds, NCGC00138783, NCG00538430 and NCG00538419

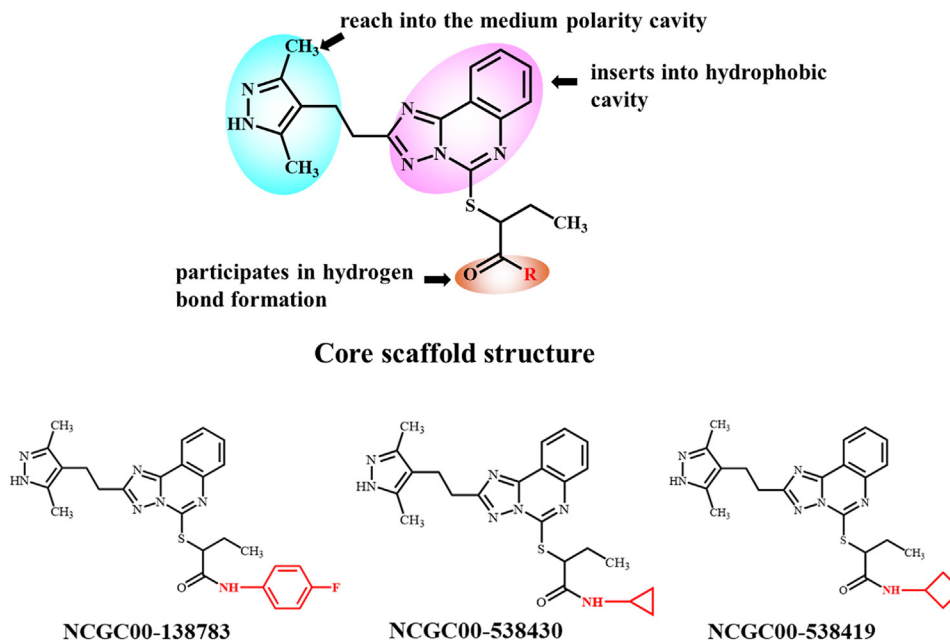


**Fig. 4.** The core scaffold structure and representative compounds of NCGC00138783 and its derivatives are shown.

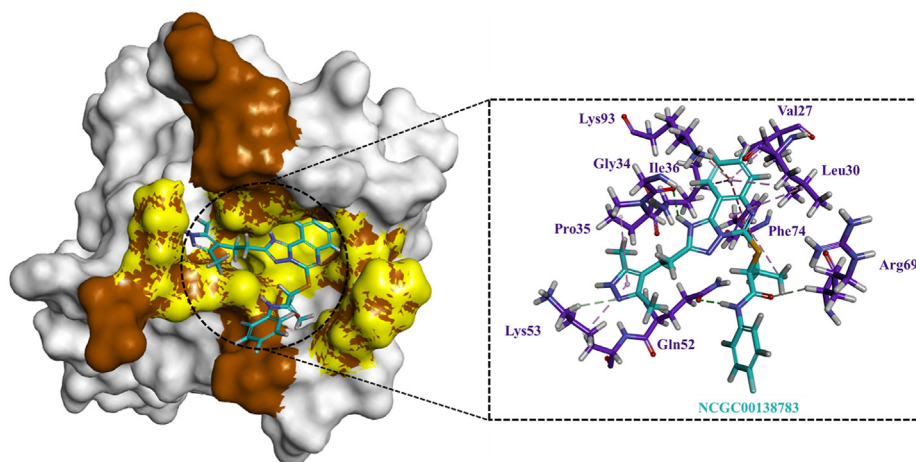


**Fig. 5.** Docking analysis of NCGC00138783 to SIRPα. The interaction area of CD47/SIRPα is colored brown, and the predicted interaction area of NCGC00138783/SIRPα is colored yellow. The interacting amino acids in SIRPα are colored purple, and the predicted interacting amino acids in NCGC00138783 is colored cyan. (For interpretation of the references to colour in this figure legend, the reader is referred to the web version of this article.)

showed antagonistic activity in both the ALPHA screening assay and LSC assay.

To facilitate the understanding of NCGC00138783 binding to CD47/SIRPα, we conducted docking experiments of NCGC00138783 docking to CD47 and SIRPα and employed the CD47/SIRPα complex (PDB ID: 2JJT) as a receptor. Consequently, we found that NCGC00138783 is more prone to bind to SIRPα than CD47 with the corresponding highest LibDock Score of 134 and 85. Furthermore, the 3,5-dimethyl-1H-pyrazolyl group, central [1,2,4] triazolo[1,5-c] quinazoline group and amide group of NCGC00138783 are predicted to form hydrogen bonds and T-stacking interactions with SIRPα, including Leu<sup>30</sup>, Gly<sup>34</sup>, Pro<sup>35</sup>, Gln<sup>52</sup>, Lys<sup>53</sup> and Lys<sup>93</sup>, which are key residues in the CD47/SIRPα interaction. The central [1,2,4] triazolo[1,5-c] quinazoline scaffold is predicted to form pi-pi stacking with Phe<sup>74</sup> and hydrogen bonding with Gly<sup>34</sup>, which makes it insert into the hydrophobic cavity. The amide group of 3,5-dimethyl-1H-pyrazolyl is predicted to form

hydrogen bonding with Gln<sup>52</sup>, which lies in the high polarity area (Fig. 5, produced by Discovery Studio2019). Above all, NCGC00138783 binds to SIRPα and occupies the key binding positions of the CD47/SIRPα interaction which is essential information for future small molecule inhibitor design and helpful for the discovery of novel inhibitors blocking the CD47/SIRPα interaction.

#### 4.2. 1,2,4-oxadiazole compounds

In a patent application, inventors from Aurigene Discovery Technologies Limited reported a series of small molecules blocking the CD47/SIRPα interaction [70]. The scaffold of these compounds is oxadiazole which can enhance macrophage-mediated phagocytosis of human lymphoma and myeloma cells, with corresponding normalized phagocytosis rates in the range of 20%–66% and 17%–77% at 10 μM. Among these small molecules, compounds 1 to 14 display comprehensive effects on both luciferase-based and

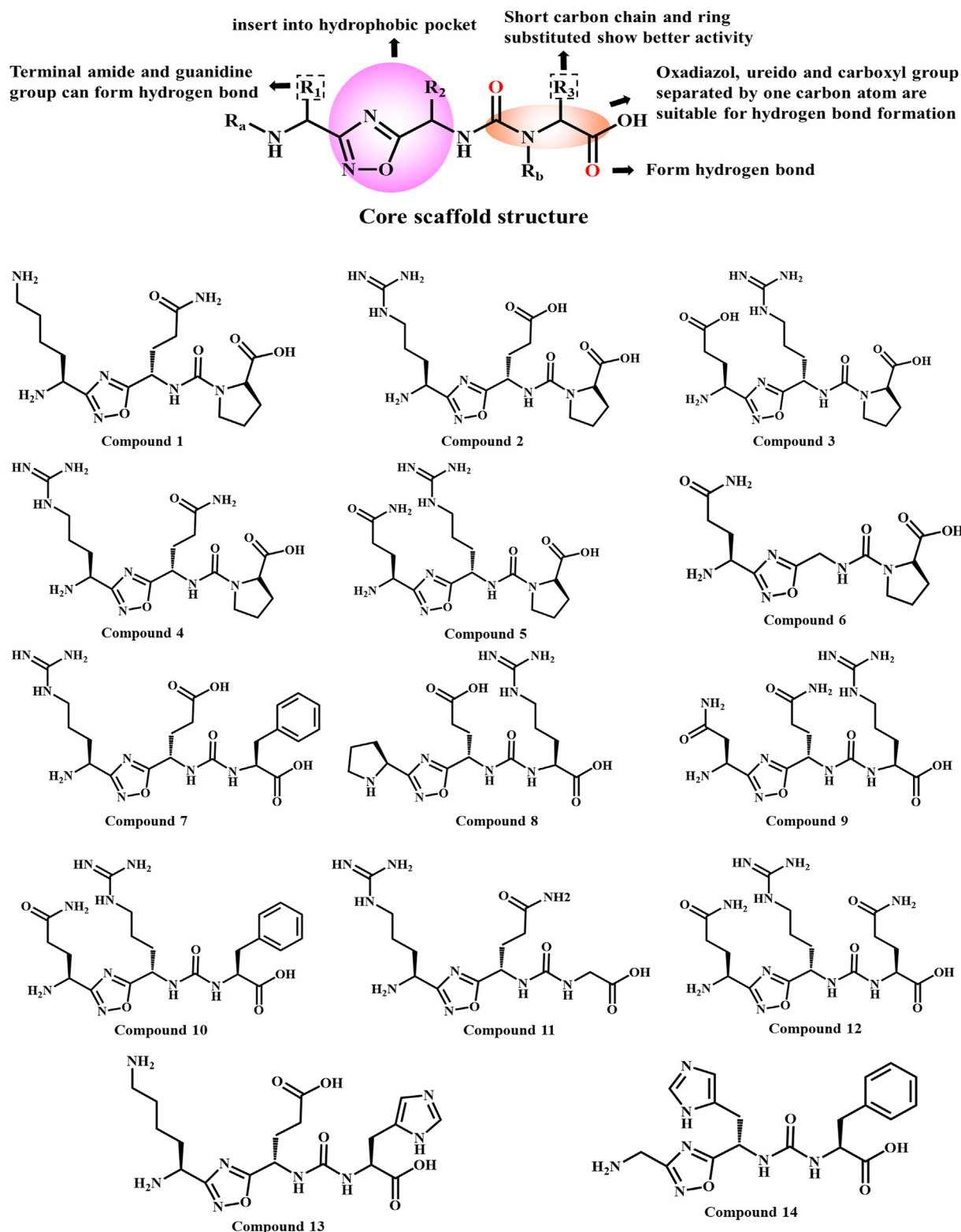
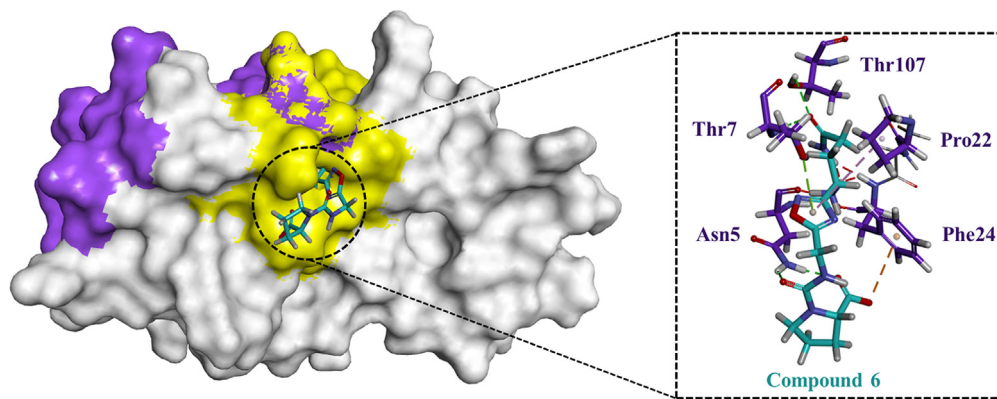


**Fig. 6.** The core scaffold structure and representative 1,2,4-oxadiazole compounds are shown.

FACS-based phagocytosis assays, and compound 6 has normalized phagocytosis rates of 66% and 74%, respectively (Fig. 6, produced by ChemDraw). Moreover, compound 6 inhibited tumor growth in a dose-dependent manner with inhibition rates of 53%, 64% and 67% at doses of 3, 10 and 30 mg/kg, respectively, in an A20 mouse model without body weight loss.

Further docking analyses of compound 6 to CD47 (PDB ID: 2JJT) by us revealed that the core 1,2,4-oxadiazole and butyramide groups insert into a hydrophobic pocket containing Trp<sup>40</sup>, Thr<sup>107</sup> and Lys<sup>6</sup> of CD47, which is the key residue in the CD47/SIRP $\alpha$  interaction. The carbonyl group of butyramide is predicted to form hydrogen bonds with Thr<sup>7</sup> and Thr<sup>107</sup>, which is near the core



**The interaction of Compound 6/CD47**

**Fig. 7.** Docking analysis of compound 6 binding to CD47. The interaction area of CD47/SIRP $\alpha$  is colored purple, and the predicted interaction area of compound 6/CD47 is colored yellow. The interacting amino acids in CD47 are colored purple, and the predicted interacting amino acids compound 6 is colored cyan. (For interpretation of the references to colour in this figure legend, the reader is referred to the web version of this article.)

CD47/SIRP $\alpha$  interaction area. Two carbonyl groups of carbamoyl proline are predicted to interact with Asn<sup>5</sup>, which is close to Lys<sup>6</sup> of CD47 (Fig. 7, produced by Discovery Studio2019). Overall, promising compound 6 could inspire the design of follow-up lead compound scaffolds, and the binding model of compound 6 to CD47 may provide information for further discovery of small molecules blocking the CD47/SIRP $\alpha$  interaction.

#### 4.3. CADD guides the design of small molecule inhibitors

Analysis of our above docking results and the published phagocytosis assays revealed the common structural characteristics of anti-CD47 compounds: (i) hydrogen bond interactions are crucial for anti-CD47 compound activity; (ii) the 2-position side chain of oxadiazol inserted into the pocket consisting of Asn<sup>5</sup>, Thr<sup>7</sup>, Pro<sup>22</sup>, Phe<sup>24</sup> and Thr<sup>107</sup> has a crucial effect on phagocytic activity; (iii) the terminal group of the oxadiazol 2-position side chain, including the amino group, carboxyl group, amide group and guanidine group, which can form hydrogen bonds with Thr<sup>7</sup> and Thr<sup>107</sup> in the pocket, exhibits higher phagocytic activity; and (iv) the oxadiazol 5-position side chain contains a terminal carboxyl group and ureido. Oxadiazol, ureido and carboxyl groups are separated by one carbon atom, which makes two carbonyl groups in suitable positions to form hydrogen bonds with Asn<sup>5</sup>; (v) the substituted short carbon chain and substituted ring alpha carbon of the terminal carboxyl group in the oxadiazol 5-position side chain can achieve better activity; (vi) central oxadiazole is needed for pi-lone pair conjugation with Thr<sup>7</sup>.

In addition, analysis of anti-SIRP $\alpha$  compounds also indicates several features: (i) hydrophobic interactions are essential for SIRP $\alpha$  binding; (ii) central quinazoline reaches a hydrophobic pocket containing Val<sup>27</sup>, Leu<sup>30</sup>, Ile<sup>36</sup>, Phe<sup>74</sup> and Lys<sup>93</sup> to form two T-stacking interactions with Phe<sup>74</sup>; and (iii) amide groups forming hydrogen bonds with Gln<sup>52</sup>, benzene, and four-membered ring- or three-membered ring- substituted amide groups show favorable antagonistic activity.

## 5. Summary and outlook

Recently, CD47/SIRP $\alpha$  inhibitors have aroused enormous interest among researchers and have been remarkably affective in cancer treatment. This field is progressing rapidly, and some mAbs targeting the CD47/SIRP $\alpha$  pathway have reached clinical phase II and phase III [71]. Notably, despite the excellent clinical perfor-

mance shown by CD47/SIRP $\alpha$  antibodies, the limitations of antibody drugs including poor tumor permeability, undesirable oral bioavailability and poor stability, hinder their clinical application [72–75]. Small-molecule inhibitors can eliminate the problems caused by antibody drugs and thus have attracted the attention of researchers and have become a promising research area.

Currently, several crystal structures of CD47/SIRP $\alpha$  and the structures of antibodies together with receptors have been published which provides guidance for the rational design of small molecule inhibitors blocking the CD47/SIRP $\alpha$  interaction. Moreover, there are two published small molecule compound categories: small molecules containing 3,5-dimethyl-1H-pyrazolyl and [1,2,4] triazolo[1,5-c] quinazoline scaffolds and small molecules containing oxadiazole scaffolds.

Unfortunately, no small molecules blocking the CD47/SIRP $\alpha$  interaction have reached clinical research yet. The shortage of target structure information limits the development of small molecule inhibitors. Excitingly, using CADD to analyze the CD47/SIRP $\alpha$  interaction will provide some crucial information for the design of small molecule inhibitors. First, CADD allows researchers to analyze the interaction between inhibitors and their receptors based on their crystal structures, which improves the understanding of the interaction process and helps to determine key information, including pocket atoms and hot spot residues. Next, CADD helps researchers to explore the interaction between inhibitors and receptors without crystal structure through docking. Here, based on the previous reports and our docking research, we conclude that Glu<sup>104</sup> and Glu<sup>106</sup> are hot spots on CD47, while Gln<sup>52</sup>, Lys<sup>53</sup> and Phe<sup>56</sup> are hot spots on SIRP $\alpha$ .

There is a limited number of small molecule inhibitors targeting the CD47/SIRP $\alpha$  pathway, which indicates the early stage of this research, but the favorable clinical results are promising. The CADD technologies will accelerate the discovery of novel inhibitors. These peptides and small molecule inhibitors will be the foundation for the design of new compounds. As it relates to drug design, the interaction area of CD47/SIRP $\alpha$  is broad. Therefore, it is crucial to identify the best binding positions for small molecules, and drug design based on these structural data will lead to the successful development of CD47/SIRP $\alpha$  inhibitors.

#### CRediT authorship contribution statement

**Bo Huang:** Conceptualization, Writing – original draft, Writing – review & editing, Visualization. **Zhaoshi Bai:** Supervision, Writ-



ing – review & editing. **Xinyue Ye:** Visualization. **Chenyu Zhou:** Resources. **Xiaolin Xie:** Visualization. **Yuejiao Zhong:** Resources. **Kejiang Lin:** Supervision, Conceptualization. **Lingman Ma:** Supervision, Writing – original draft, Writing – review & editing.

### Declaration of Competing Interest

The authors declare that they have no known competing financial interests or personal relationships that could have appeared to influence the work reported in this paper.

### Acknowledgements

This work was supported by grants from the National Natural Science Foundation (81903642), China Postdoctoral Science Foundation (2020M681528), Postdoctoral Science Foundation of Jiangsu Province (2021K369C) and Jiangsu Cancer Hospital Postdoctoral Science Foundation (SZL202015).

### References

- Wang H, Yin Y, Wang P, Xiong C, Huang L, Li S, et al. Current situation and future usage of anticancer drug databases. *Apoptosis* 2016;21:778–94.
- Couzin-Frankel J. Cancer immunotherapy. *Science* 2013;342:1432–3.
- Riley RS, June CH, Langer R, Mitchell MJ. Delivery technologies for cancer immunotherapy. *Nat Rev Drug Discov* 2019;18:175–96.
- Rosenberg SA. IL-2: the first effective immunotherapy for human cancer. *J Immunol* 2014;192:5451–8.
- Waldman AD, Fritz JM, Lenardo MJ. A guide to cancer immunotherapy: from T cell basic science to clinical practice. *Nat Rev Immunol* 2020;20:651–68.
- Khair DO, Bax HJ, Mele S, Crescioli S, Pellizzari G, Khiabany A, et al. Combining immune checkpoint inhibitors: established and emerging targets and strategies to improve outcomes in melanoma. *Front Immunol* 2019;10.
- Zitvogel L, Tesniere A, Kroemer G. Cancer despite immunosurveillance: immunoselection and immunosubversion. *Nat Rev Immunol* 2006;6:715–27.
- Pardoll DM. The blockade of immune checkpoints in cancer immunotherapy. *Nat Rev Cancer* 2012;12:252–64.
- Sadreddini S, Baradaran B, Aghebati-Maleki A, Sadreddini S, Shanebandi D, Fotouhi A, et al. Immune checkpoint blockade opens a new way to cancer immunotherapy. *J Cell Physiol* 2019;234:8541–9.
- Veillette A, Chen J. SIRP alpha-CD47 immune checkpoint blockade in anticancer therapy. *Trends Immunol* 2018;39:173–84.
- Lipson EJ, Drake CG. Ipilimumab: an anti-CTLA-4 antibody for metastatic melanoma. *Clin Cancer Res* 2011;17:6958–62.
- Postow MA, Callahan MK, Wolchok JD. Immune checkpoint blockade in cancer therapy. *J Clin Oncol* 2015;33:1974–82.
- Alsaab HO, Sau S, Alzhrani R, Tatiparti K, Bhise K, Kashaw SK, et al. PD-1 and PD-L1 checkpoint signaling inhibition for cancer immunotherapy: mechanism, combinations, and clinical outcome. *Front Pharmacol* 2017;8:561.
- Qin S, Xu L, Yi M, Yu S, Wu K, Luo S. Novel immune checkpoint targets: moving beyond PD-1 and CTLA-4. *Mol Cancer* 2019;18.
- Ratner L, Waldmann TA, Janakiram M, Brammer JE. Rapid progression of adult T-cell leukemia-lymphoma after PD-1 inhibitor therapy. *N Engl J Med* 2018;378:1947–8.
- Limagne E, Richard C, Thibaudin M, Fumet J-D, Trunzter C, Lagrange A, et al. Tim-3/galectin-9 pathway and mMDS control primary and secondary resistances to PD-1 blockade in lung cancer patients. *Oncoimmunology* 2019;8.
- Matlung HL, Szilagy K, Barclay NA, van den Berg TK. The CD47-SIRPalpha signaling axis as an innate immune checkpoint in cancer. *Immunol Rev* 2017;276:145–64.
- Murata Y, Saito Y, Kotani T, Matozaki T. CD47-signal regulatory protein signaling system and its application to cancer immunotherapy. *Cancer Sci* 2018;109:2349–57.
- Lindberg FP, Gresham HD, Schwarz E, Brown EJ. Molecular cloning of Integrin-Associated Protein: an immunoglobulin family member with multiple membrane spanning domains implicated in  $\alpha v \beta 3$ -dependent ligand binding. *J Cell Biol* 1993;123:485–96.
- Majeti R, Chao MP, Alizadeh AA, Pang WW, Jaiswal S, Gibbs Jr KD, et al. CD47 is an adverse prognostic factor and therapeutic antibody target on human acute myeloid leukemia stem cells. *Cell* 2009;138:286–99.
- Chao MP, Alizadeh AA, Tang C, Myklebust JH, Varghese B, Gill S, et al. Anti-CD47 antibody synergizes with rituximab to promote phagocytosis and eradicate non-Hodgkin lymphoma. *Cell* 2010;142:699–713.
- Zhang W, Huang Q, Xiao W, Zhao Y, Pi J, Xu H, et al. Advances in anti-tumor treatments targeting the CD47/SIRP alpha axis. *Front Immunol* 2020;11.
- Brown EJ, Frazier WA. Integrin-associated protein (CD47) and its ligands. *Trends Cell Biol* 2001;11:130–5.
- Adams S, van der Laan LJW, Vernon-Wilson E, de Lavalette CR, Dopp EA, Dijkstra CD, et al. Signal-regulatory protein is selectively expressed by myeloid and neuronal cells. *J Immunol* 1998;161:1853–9.
- Seiffert M, Cant C, Chen ZJ, Rappold I, Brugger W, Kanz L, et al. Human signal-regulatory protein is expressed on normal, but not on subsets of leukemic myeloid cells and mediates cellular adhesion involving its counterreceptor CD47. *Blood* 1999;94:3633–43.
- Logtenberg MEW, Scheeren FA, Schumacher TN. The CD47-SIRP alpha immune checkpoint. *Immunity* 2020;52:742–52.
- Kharitonov A, Chen ZJ, Sures I, Wang HY, Schilling J, Ullrich A. A family of proteins that inhibit signalling through tyrosine kinase receptors. *Nature* 1997;386:181–6.
- Chao MP, Jaiswal S, Weissman-Tsakamoto R, Alizadeh AA, Gentles AJ, Volkmer J, et al. Calreticulin is the dominant pro-phagocytic signal on multiple human cancers and is counterbalanced by CD47. *Sci Transl Med* 2010;2.
- Liu M, O'Connor RS, Trefely S, Graham K, Snyder NW, Beatty GL. Metabolic rewiring of macrophages by CpG potentiates clearance of cancer cells and overcomes tumor-expressed CD47-mediated 'don't-eat-me' signal. *Nat Immunol* 2019;20:265–75.
- Weiskopf K, Jahchan NS, Schnorr PJ, Cristea S, Ring AM, Maute RL, et al. CD47-blocking immunotherapies stimulate macrophage-mediated destruction of small-cell lung cancer. *J Clin Invest* 2016;126:2610–20.
- Lian S, Xie R, Ye Y, Xie X, Li S, Lu Y, et al. Simultaneous blocking of CD47 and PD-L1 increases innate and adaptive cancer immune responses and cytokine release. *Biomedicine* 2019;42:281–95.
- Kiss B, van den Berg NS, Ertsey R, McKenna K, Mach KE, Zhang CA, et al. CD47-targeted near-infrared photoimmunotherapy for human bladder cancer. *Clin Cancer Res* 2019;25:3561–71.
- Chao MP, Takimoto CH, Feng DD, McKenna K, Gip P, Liu J, et al. Therapeutic targeting of the macrophage immune checkpoint CD47 in myeloid malignancies. *Front Oncol* 2020;9.
- Brierley CK, Staves J, Roberts C, Johnson H, Vyas P, Goodnough LT, et al. The effects of monoclonal anti-CD47 on RBCs, compatibility testing, and transfusion requirements in refractory acute myeloid leukemia. *Transfusion* 2019;59:2248–54.
- Schurich CM, Roelli MA, Forster S, Wasmer M-H, Bruhl F, Maire RS, et al. Targeting CD47 in anaplastic thyroid carcinoma enhances tumor phagocytosis by macrophages and is a promising therapeutic strategy. *Thyroid* 2019;29:979–92.
- Advani R, Flinn I, Popplewell L, Forero A, Bartlett NL, Ghosh N, et al. CD47 Blockade by Hu5F9-G4 and Rituximab in Non-Hodgkin's Lymphoma. *N Engl J Med* 2018;379:1711–21.
- Jain S, Van Scoyk A, Morgan EA, Matthews A, Stevenson K, Newton G, et al. Targeted inhibition of CD47-SIRP alpha requires Fc-Fc gamma R interactions to maximize activity in T-cell lymphomas. *Blood* 2019;134:1430–40.
- Ansell SM, Maris MB, Lesokhin AM, Chen RW, Flinn IW, Sawas A, et al. Phase I Study of the CD47 Blocker TTI-621 in Patients with Relapsed or Refractory Hematologic Malignancies. *American Association for Cancer Research*; 2021.
- Zhang X, Wang Y, Fan J, Chen W, Luan J, Mei X, et al. Blocking CD47 efficiently potentiated therapeutic effects of anti-angiogenic therapy in non-small cell lung cancer. *J Immunother Cancer* 2019;7.
- Puro RJ, Bouchlaka MN, Hiebsch RR, Capoccia BJ, Donio MJ, Manning PT, et al. Development of AO-176, a next-generation humanized anti-CD47 antibody with novel anticancer properties and negligible red blood cell binding. *Mol Cancer Ther* 2020;19:835–46.
- Kaur S, Elkahoul AG, Singh SP, Chen Q-R, Meerzaman DM, Song T, et al. A function-blocking CD47 antibody suppresses stem cell and EGF signaling in triple-negative breast cancer. *Oncotarget* 2016;7:10133–52.
- Sikic BI, Lakhani N, Patnaik A, Shah SA, Chandana SR, Rasco D, et al. First-in-human, first-in-class phase I trial of the anti-CD47 antibody Hu5F9-G4 in patients with advanced cancers. *J Clin Oncol* 2019;37:946.
- Li K, Tian H. Development of small-molecule immune checkpoint inhibitors of PD-1/PD-L1 as a new therapeutic strategy for tumour immunotherapy. *J Drug Target* 2019;27:244–56.
- Xu T, Zheng W, Huang R. High-throughput screening assays for SARS-CoV-2 drug development: Current status and future directions. *Drug Discovery Today* 2021.
- Blay V, Tolani B, Ho SP, Arkin MR. High-Throughput Screening: today's biochemical and cell-based approaches. *Drug Discovery Today* 2020;25:1807–21.
- Clare RH, Bardelle C, Harper P, Hong WD, Borjesson U, Johnston KL, et al. Industrial scale high-throughput screening delivers multiple fast acting macrofilaricides. *Nat Commun* 2019;10.
- Lima MNN, Neves BJ, Cassiano GC, Gomes MN, Tomaz KCP, Ferreira LT, et al. Chalcones as a basis for computer-aided drug design: innovative approaches to tackle. *Fut Med Chem* 2019;11:2635–46.
- Kumar V, Kumar R, Parate S, Yoon S, Lee G, Kim D, et al. Identification of ACK1 inhibitors as anticancer agents by using computer-aided drug designing. *J Mol Struct* 2021;1235.
- Clark DE. What has computer-aided molecular design ever done for drug discovery? *Expert Opin Drug Discov* 2006;1:103–10.
- Macalino SJY, Gosu V, Hong S, Choi S. Role of computer-aided drug design in modern drug discovery. *Arch Pharmacol Res* 2015;38:1686–701.
- Hatherley D, Graham SC, Turner J, Harlos K, Stuart DI, Barclay AN. Paired receptor specificity explained by structures of signal regulatory proteins alone and complexed with CD47. *Mol Cell* 2008;31:266–77.

- [52] Hatherley D, Harlos K, Dunlop DC, Stuart DI, Barclay AN. The structure of the macrophage signal regulatory protein alpha (SIRP alpha) inhibitory receptor reveals a binding face reminiscent of that used by T cell receptors. *J Biol Chem* 2007;282:14567–75.
- [53] Weiskopf K, Ring AM, Ho CCM, Volkmer J-P, Levin AM, Volkmer AK, et al. Engineered SIRP alpha variants as immunotherapeutic adjuvants to anticancer antibodies. *Science* 2013;341:88–91.
- [54] Pietsch EC, Dong J, Cardoso R, Zhang X, Chin D, Hawkins R, et al. Anti-leukemic activity and tolerability of anti-human CD47 monoclonal antibodies. *Blood Cancer J* 2017;7.
- [55] Wu Z, Weng L, Zhang T, Tian H, Fang L, Teng H, et al. Identification of Glutaminyl Cyclase isoenzyme isoQC as a regulator of SIRPalpha-CD47 axis. *Cell Res* 2019;29:502–5.
- [56] Logtenberg MEW, Jansen JHM, Raaben M, Toebes M, Franke K, Brandsma AM, et al. Glutaminyl cyclase is an enzymatic modifier of the CD47- SIRPalpha axis and a target for cancer immunotherapy. *Nat Med* 2019;25:612–9.
- [57] Wang H, Sun Y, Zhou X, Chen C, Jiao L, Li W, et al. CD47/SIRP alpha blocking peptide identification and synergistic effect with irradiation for cancer immunotherapy. *J Immunother Cancer* 2020;8.
- [58] Hatherley D, Lea SM, Johnson S, Barclay AN. Polymorphisms in the human inhibitory signal-regulatory protein alpha do not affect binding to its ligand CD47\*. *J Biol Chem* 2014;289:10024–8.
- [59] Rodriguez PL, Harada T, Christian DA, Pantano DA, Tsai RK, Discher DE. Minimal “Self” peptides that inhibit phagocytic clearance and enhance delivery of nanoparticles. *Science* 2013;339:971–5.
- [60] Xu H, Wang X. Polypeptide RS-17 with anti-CD47 immune checkpoint antagonistic activity and application thereof. 2020.
- [61] Yamagishi Y, Shoji I, Miyagawa S, Kawakami T, Katoh T, Goto Y, et al. Natural product-like macrocyclic N-methyl-peptide inhibitors against a ubiquitin ligase uncovered from a ribosome-expressed de novo library. *Chem Biol* 2011;18:1562–70.
- [62] Hazama D, Yin Y, Murata Y, Matsuda M, Okamoto T, Tanaka D, et al. Macrocyclic peptide-mediated blockade of the CD47-SIRP alpha Interaction as a potential cancer immunotherapy. *Cell Chem Biol* 2020;27:1181.
- [63] Nakaishi A, Hirose M, Yoshimura M, Oneyama C, Saito K, Kuki N, et al. Structural insight into the specific interaction between murine SHPS-1/SIRP alpha and its ligand CD47. *J Mol Biol* 2008;375:650–60.
- [64] Gao Y, Li Y, Zhai W, Qi Y, Wang H. Sirpa protein affinity cyclic peptide and application thereof. China: Zhengzhou University; 2020.
- [65] Burgess TL, Amason JD, Rubin JS, Duveau DY, Lamy L, Roberts DD, et al. A homogeneous SIRP alpha-CD47 cell-based, ligand-binding assay: Utility for small molecule drug development in immuno-oncology. *PLoS ONE* 2020;15.
- [66] Miller TW, Amason JD, Garcin ED, Lamy L, Dranchak PK, Macarthur R, et al. Quantitative high-throughput screening assays for the discovery and development of SIRP alpha-CD47 interaction inhibitors. *PLoS ONE* 2019;14.
- [67] Courageot M-P, Duca L, Martiny L, Devarenne-Charpentier E, Morjani H, El Btaouri H. Thrombospondin-1 receptor CD47 overexpression contributes to P-glycoprotein-mediated multidrug resistance against doxorubicin in thyroid carcinoma FTC-133 cells. *Front Oncol* 2020;10.
- [68] Bissinger R, Petkova-Kirova P, Mykhailova O, Oldenborg P-A, Novikova E, Donkor DA, et al. Thrombospondin-1/CD47 signaling modulates transmembrane cation conductance, survival, and deformability of human red blood cells. *Cell Commun Signal* 2020;18.
- [69] Wang Q, Onuma K, Liu C, Wong H, Bloom MS, Elliott EE, et al. Dysregulated integrin alpha(V)beta(3) and CD47 signaling promotes joint inflammation, cartilage breakdown, and progression of osteoarthritis. *JCI Insight* 2019;4.
- [70] Sasikumar Pottayil Govindan Nair RM, Naremaddepalli Seetharamaiah Setty Sudarshan, Chennakrishnareddy Gundala. 1,2,4-Oxadiazole Compounds as Inhibitors of CD47 Signalling, India2019.
- [71] Bewersdorf JP, Risk-Adapted ZAM. Individualized Treatment Strategies of Myelodysplastic Syndromes (MDS) and Chronic Myelomonocytic Leukemia (CMML). *Cancers (Basel)* 2021;13.
- [72] Sifniotis V, Cruz E, Eroglu B, Kayser V. Current Advancements in Addressing Key Challenges of Therapeutic Antibody Design, Manufacture, and Formulation. *Antibodies (Basel, Switzerland)*. 2019;8.
- [73] Ren T, Tan Z, Ehamparanathan V, Lewandowski A, Ghose S, Li ZJ. Antibody disulfide bond reduction and recovery during biopharmaceutical process development – A review. *Biotechnol Bioeng* 2021.
- [74] Kitten O, Martineau P. Antibody alternative formats: antibody fragments and new frameworks. *M S-Med Sci* 2020;35:1092–7.
- [75] Ma H, O’Fagain C, O’Kennedy R. Antibody stability: A key to performance - Analysis, influences and improvement. *Biochimie* 2020;177:213–25.